

Article

Extraction of Vanadium from the Spent Residuum Hydroprocessing Catalysts by Fenton-like Reaction Followed with Alkaline Leaching

Yuefen Lv¹, Ge Zhao², Cailong Shen^{3,4}, Yanzhen Chen^{3,4}, Yiqun Fan¹, Guangji Zhang^{3,4,*} and Chao Yang^{3,4,*}

- ¹ State Key Laboratory of Materials-Oriented Chemical Engineering, College of Chemical Engineering, Nanjing Tech University, Nanjing 211816, China; yiqunfan@njtech.edu.com (Y.F.)
- ² School of Chemical Engineering, China University of Mining and Technology (Beijing), Beijing 100083, China
- ³ CAS Key Laboratory of Green Process and Engineering, Institute of Process Engineering, Chinese Academy of Sciences, Beijing 100190, China; chenyanzhen@ipe.ac.cn (Y.C.)
- ⁴ School of Chemical Engineering, University of Chinese Academy of Sciences, Beijing 100049, China
- * Correspondence: gjzhang@ipe.ac.cn (G.Z.); chaoyang@ipe.ac.cn (C.Y.)

Abstract: Spent residuum hydroprocessing (RHDP) catalysts are hazardous waste bearing high-content vanadium and large amounts of oily pollutants. In this paper, a process featuring a Fenton-like reaction and alkaline leaching was proposed to recover vanadium from spent RHDP catalysts. In the first step, a Fenton-like reaction using peroxide was conducted to degrade the oily pollutants and make the surface of the spent catalyst becomes hydrophilic. In the second step, the vanadium-containing deposit on the catalyst was leached with 0.5 M Na₂S₂O₈ at 70 °C for transforming vanadium sulfide to oxide in 5 h. In the last step, alkaline leaching was employed to dissolve vanadium from the oxidizing residue at 80 °C for 1 h. It was found that the accumulated leaching efficiency of vanadium can reach up to 90.92%, and only a small part of aluminum and sulfur was dissolved. These results indicated that this combined process can extract vanadium selectively from spent residuum hydroprocessing catalysts under a relatively mild condition.



Citation: Lv, Y.; Zhao, G.; Shen, C.; Chen, Y.; Fan, Y.; Zhang, G.; Yang, C. Extraction of Vanadium from the Spent Residuum Hydroprocessing Catalysts by Fenton-like Reaction Followed with Alkaline Leaching. *Processes* **2023**, *11*, 2021. <https://doi.org/10.3390/pr11072021>

Academic Editors: Patrick Dunlop, Efthalia Chatzisyemon and Leónidas Pérez Estrada

Received: 11 May 2023
Revised: 13 June 2023
Accepted: 23 June 2023
Published: 6 July 2023



Copyright: © 2023 by the authors. Licensee MDPI, Basel, Switzerland. This article is an open access article distributed under the terms and conditions of the Creative Commons Attribution (CC BY) license (<https://creativecommons.org/licenses/by/4.0/>).

Keywords: spent residuum hydroprocessing catalyst; vanadium; Fenton-like reaction; oil removal; alkali leaching

1. Introduction

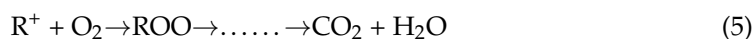
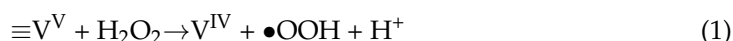
Petroleum hydroprocessing catalysts commonly consist of an active component and carrier, which is generally prepared via the impregnation method by loading a salt solution containing the active component Ni/Mo on the Al₂O₃ [1]. Crude oils usually contain large amounts of vanadium–nickel porphyrin compounds from animal carcasses [2,3]. During the hydrotreating process of the residuum, vanadium in the feedstock is gradually deposited on the catalyst as sulfides, and the vanadium content in spent catalysts can even exceed 10% [4–7], which is higher than that of natural minerals. Vanadium is harmful to the environment, but it is also a useful metal. Therefore, RHDP catalysts can be considered a potential secondary source for obtaining vanadium [8,9]. On the other hand, spent catalysts have been classified as hazardous waste by many countries and organizations [10,11]. Therefore, the extraction of vanadium from spent RHDP catalysts is of great importance from the perspective of environmental protection and resource utilization.

Pyrometallurgy, hydrometallurgy, and a combination of both processes are the main routes to recover valuable metals from spent RHDP catalysts [12]. In the pyrometallurgical process, the release of harmful gases and the required high energy consumption result in poor economic compensation during the recycling of spent catalysts. Hydrometallurgy is the preferred method in most cases because of its low energy consumption, no gas emissions, and high metal-recovery efficiency. In the hydrometallurgical process, the oil

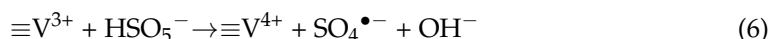
covering the surface of the spent RHDP catalyst has to be removed before the extraction of the valuable metals. Roasting is a simple and effective way to remove the oil, and in this process, the metal sulfides in the spent catalyst can be converted to metal oxides. This is a beneficial transformation for metal recovery [13]. However, the roasting process will lead to harmful gases emission and impurity generation caused by oil combustion [14,15]. Washing with organic solvents or surfactants can be performed at low temperatures without harmful gas emissions and impurity generation. Nevertheless, how to dispose of organic waste liquids is a challenging problem. Vacuum pyrolysis can remove the oil by heating and volatilizing, but this process requires complex equipment and severe conditions.

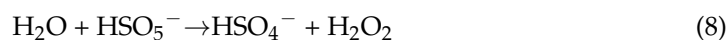
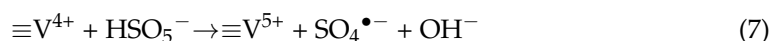
Zhang et al. [16] explored an integrated selective process to recover valuable metals from spent catalysts. Oily catalysts were roasted at 400 °C, and nickel, molybdenum, and vanadium were selectively leached with ammonia. In the second leaching step, vanadium was leached with ammonia at pH 12, and the leaching efficiency of vanadium reached over 97.13%. This route is highly selective, but the environmental pollution caused by roasting and ammonia limits its application. Yue Yang et al. [17] proposed a simple washing method to successfully remove oil from oily spent catalysts using an alkaline SDS solution. The de-oiled catalyst was roasted at 500 °C, and the high leaching efficiency of molybdenum with 1.6 M Na₂CO₃ solution could be achieved. This study concluded that roasting after oil removal can effectively avoid the problem of uncontrollable system temperature and spinel compound generation to some extent, but how to dispose of the resulting oil-loaded eluents was not described. Mishra et al. [18] reported the recovery of metals from petroleum waste catalysts containing Ni, V, and Mo using a solvent extraction-leaching method. It was found that after acetone-carbon disulfide washing, the leaching efficiency of V can reach more than 95% in 1 M H₂SO₄ solution. This method has a high metal recovery efficiency, but treating large amounts of oil-containing organic waste liquid is a challenging problem. In a word, the environmental damage caused by both hazardous gases and organic waste streams containing oil cannot be ignored. Developing a novel environmentally friendly recovery process for de-oiling and metal extraction of spent RHDP catalysts is crucial.

Recently, it has been reported that vanadium(V) in many compounds, such as V₂O₅ [19] and FeVO₄ [20], could catalyze the oxidation of various organic and inorganic compounds via a Fenton-like pathway in the presence of H₂O₂. Deng et al. [21] found that FeVO₄ has higher catalytic activity than α-Fe₂O₃, Fe₃O₄, and γ-FeOOH in the oxidative degradation of orange II. The activation of H₂O₂ occurs by both Fe (III) and V(V) in FeVO₄. The reaction of hydrocarbon oxidation may be as follows:



Lai et al. [22] found that the activated persulfate system exhibited extraordinary oxidation ability for carbamazepine (CBZ) contaminants. Dithionite (DNT) can reduce the vanadium valence state, and the reduced vanadium significantly accelerates the Peroxy-monosulfate (PMS) reactions to generate reactive oxygen species (ROS). These reactions can be written as follows:





ROS can further attack the CBZ intermediates and mineralize them to CO₂ and H₂O. Moreover, Liu et al. [23] suggested that advanced oxidation can also be utilized for the oxidative leaching of metalliferous sulfide minerals. Sodium persulfate can maintain a redox potential of 2.8 eV over a wide pH range. Its oxidation capacity is higher than NaClO₃ and H₂O₂. It has been shown [24] that sodium persulfate, under acidic conditions, can oxidize low-valent metal sulfides to high-valent metal ions, which are readily dissolved in the leaching solution.

This work achieved the continuous recovery of metallic vanadium from spent RHDP catalysts (Ni-Mo-V/Al₂O₃) by Fenton-like oxidation and alkaline leaching. Briefly, the residual oil was removed by H₂O₂ Fenton-like oxidation, and the sulfide phase of the metallic species was converted using Na₂S₂O₈. Vanadium deposited on the surface of the porous Al₂O₃ carrier was rapidly leached directly from the spent RHDP catalyst by an alkaline solution. The effects of Na₂S₂O₈ concentration, reaction temperature, initial pH, and reaction time on vanadium-leaching efficiency were investigated in detail. The proposed route can achieve the pretreatment and recovery of spent RHDP catalysts under relatively mild conditions, which is significant in environmental protection and resource utilization.

2. Experimental

2.1. Materials and Reagents

The RHDP spent catalyst was provided by an oil refinery in Nanjing, Jiangsu Province. It was obtained from the Residuum Hydroprocessing Unit which has run for one year. A portion of the raw spent RHDP catalyst was crushed and ground; another part of the raw waste RHDP catalyst was washed with acetone and roasted in a muffle furnace at 800 °C, respectively. The XRF information on the surface of the raw spent catalyst is shown in Table 1. The XRF shows that the spent residuum hydroprocessing catalyst consists of Ni/Mo active components and an Al₂O₃ carrier and a large amount of deposited vanadium sulfide. The results of N₂ adsorption-desorption experiments showed that the specific surface area (SSA) of the finely ground spent catalyst particles was 21.12 m²/g, the total pore volume (TPV) was 0.058 mL/g, and the average pore diameter (APD) was 5.46 nm. The XRD pattern (Figure 1) showed that the V₂S₃ is the major component of the spent catalyst. The chemical reagents used in the tests included sulfuric acid, hydrochloric acid, hydrogen peroxide, and sodium persulphate. All reagents are of analytical grade. All the aqueous solutions were prepared using deionized water.

Table 1. Properties of catalysts before de-oiling.

Catalyst Properties	Catalyst Composition, wt%
	Raw Sample
S	17.92
V	15.75
Ni	5.36
Mo	1.58
Al	11.15

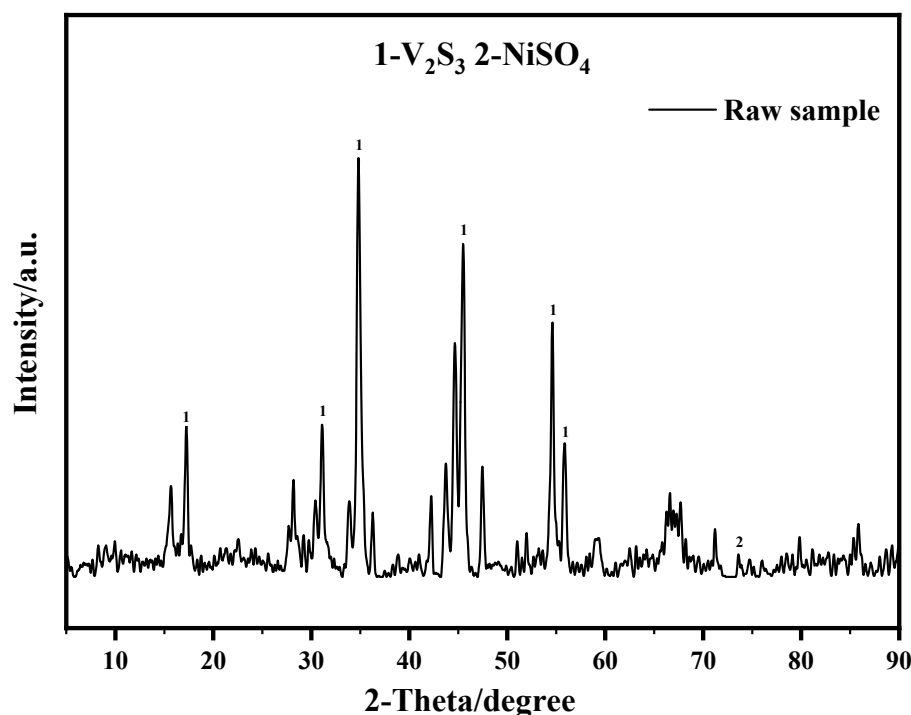


Figure 1. XRD patterns of the raw spent RHDP catalyst.

2.2. Experimental Procedures

De-oiling experiments were carried out with different concentrations of H_2O_2 solution in a three-neck flask. The leaching experiments were carried out in a 500 mL three-neck flask equipped with a magnetic agitator and a reflux condenser to recycle water and dissolution reagents during evaporation. A water bath was designated to provide the desired temperature. In this study, a two-stage oxidation-alkali leaching was employed to leach vanadium.

In the oxidizing leaching, the optimal experimental conditions were determined by studying the effects of $Na_2S_2O_8$ concentration, initial pH, reaction temperature, and reaction time on the leaching efficiency. In the alkaline-leaching step, the solution pH, reaction temperature, and reaction time were the variables initially optimized according to the previous step. A 50:1 liquid-to-solid ratio was used for all experiments. The metal leaching efficiency (R) was calculated according to Equation (8).

$$R = \frac{c \times V}{wt\% \times m} \times 100\% \quad (9)$$

where c was the concentration (mg/L) of metal ions in the leachate, V is the volume (mL) of leachate, $wt\%$ is the mass fraction of metal in the spent catalyst, and m is the mass (g) of spent catalyst.

2.3. Analytical Methods

The elemental content of the spent RHDP catalyst and the leaching residue was analyzed using an X-ray fluorescence spectrometer (XRF, AXIOS max). The textural properties of the raw spent catalyst, including specific surface area (SSA), total pore volume (TPV), and average pore diameter (APD), were determined by nitrogen physisorption (AutoChem II 2920). The organic substances in the spent catalyst were examined using Fourier transform infrared spectroscopy (FT-IR, NICOLET iS 50). The surface morphology and composition of the raw spent catalyst and the de-oiled spent catalyst were examined using a scanning electron microscope with energy-dispersive spectroscopy (SEM-EDS, JSM-7001F+INCA X-MAX); The pH of the aqueous solution was monitored using a pH meter

(FE-20). The concentration of metal ions in the leachate was determined by inductively coupled plasma atomic emission spectrometry (ICP-AES, Agilent 5800VDV).

3. Result and Discussion

3.1. Oil Removal Using H_2O_2

As shown in Figure 2, the SEM image shows that the surface of the raw spent catalyst is covered with small particles. After de-oiling, it can be seen in Figure 2b that the previous spherical buildup has disappeared and the surface of the spent catalyst has become loose, and a relatively flat surface is exposed. Some researchers reported that V_2S_3 is an acid-soluble metal sulfide and elemental sulfur is an oxidation product [25]. However, there was no elemental sulfur that can be detected by SEM and EDS of the oil removal samples. This result may be attributed to the fact that most of the H_2O_2 is depleted in the Fenton-like oxidation for oil removal and the remaining H_2O_2 is insufficient to oxidize the V_2S_3 to elemental sulfur.

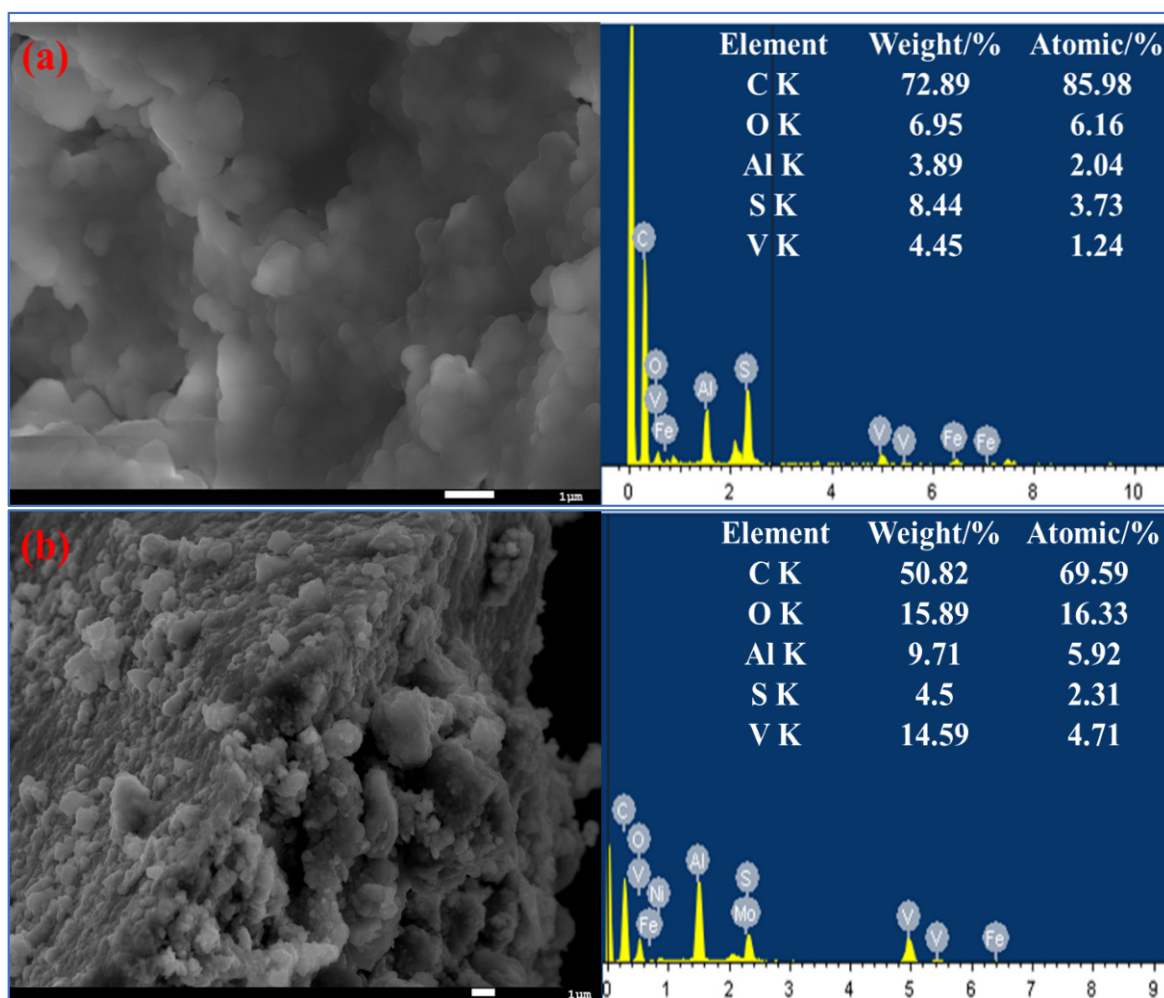


Figure 2. SEM images of the spent residuum hydroprocessing catalysts before and after de-oiling and the corresponding EDS data: (a) raw sample; (b) H_2O_2 de-oiling sample.

The corresponding EDS data showed that the C content of the spent catalyst samples decreased, and the content of other elements, such as O, Al, and vanadium, increased after the de-oiling treatment.

The results of the drop contact angle of ultrapure water on the compressed spent catalyst disk surface are shown in Figure 3. The contact angle of the raw spent catalyst is 147.3° , which shows that the raw spent catalyst has a hydrophobic surface. After oil

removal, the surface of the spent catalyst becomes hydrophilic, and the drop contact angle is 88.9° . This transformation is beneficial to metal leaching.

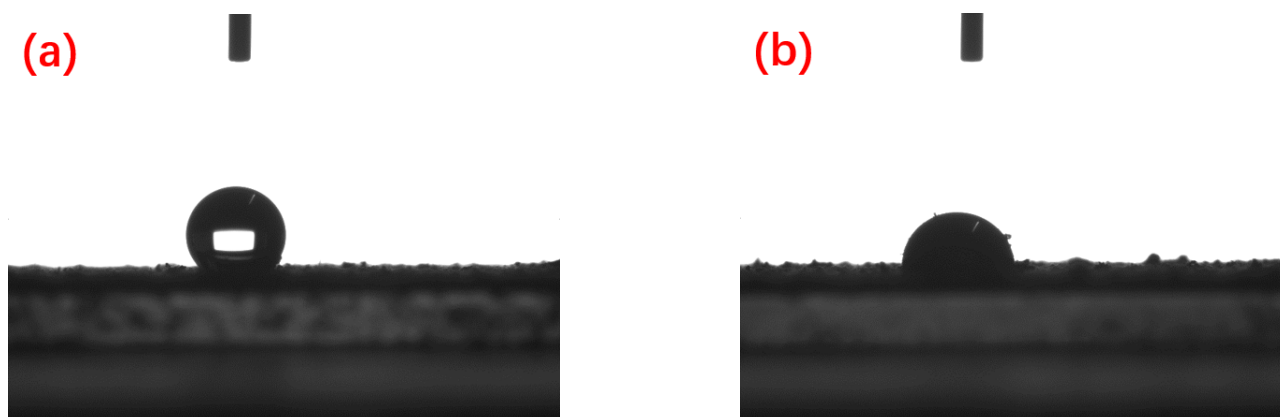


Figure 3. Drop contact angle images of the samples: (a) spent RDPH catalyst; (b) H_2O_2 de-oiling sample.

The corresponding FT-IR spectra of the samples after de-oiling in various ways are shown in Figure 4. It can be found that the C-H vibration absorption peaks of all the samples were significantly weakened after de-oiling. This result indicates that roasting, acetone washing, and H_2O_2 oxidizing all can remove hydrocarbons in the spent catalyst effectively.

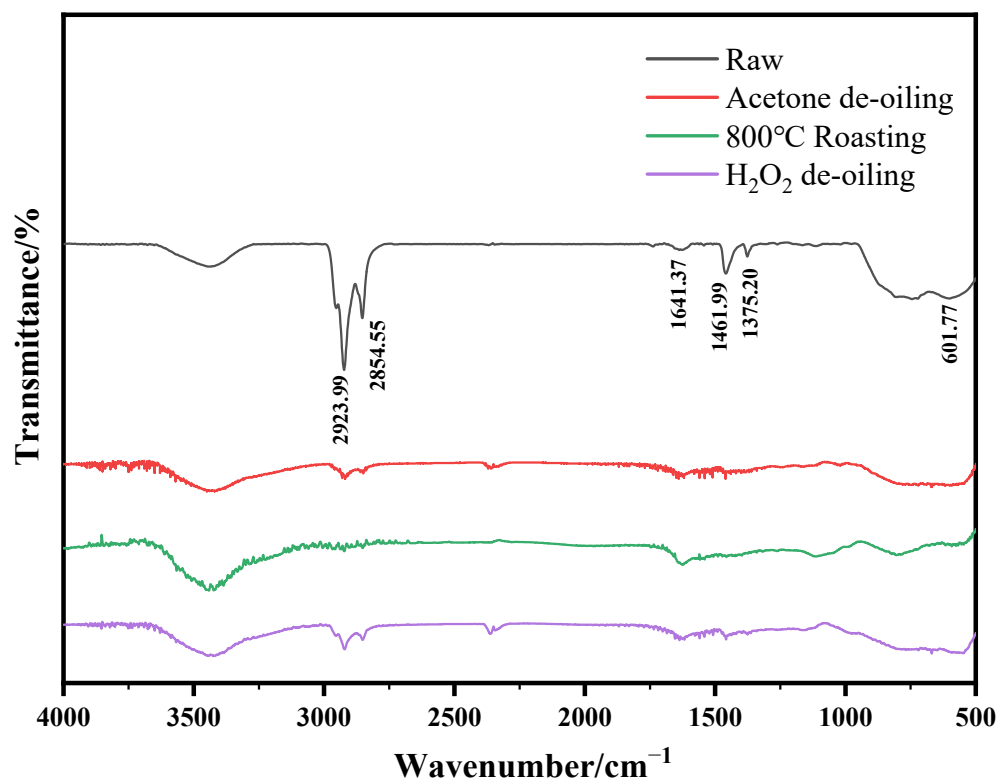


Figure 4. FT-IR spectra of the spent RDHP catalysts after different treatments.

The XRD patterns (Figure 5) showed that the acetone-washed and H_2O_2 de-oiled samples did not show any new diffraction peaks. In contrast, V_2O_3 , NiV_3O_8 , and NiV_2O_4 diffraction peaks were identified in the XRD patterns of the 800°C roasting sample. This result could illustrate that high-temperature roasting can transform metal sulfides into

metal oxides, but it also produces some new phases. From these results, it can be seen that H_2O_2 de-oiling can achieve a considerable de-oiling effect under mild conditions.

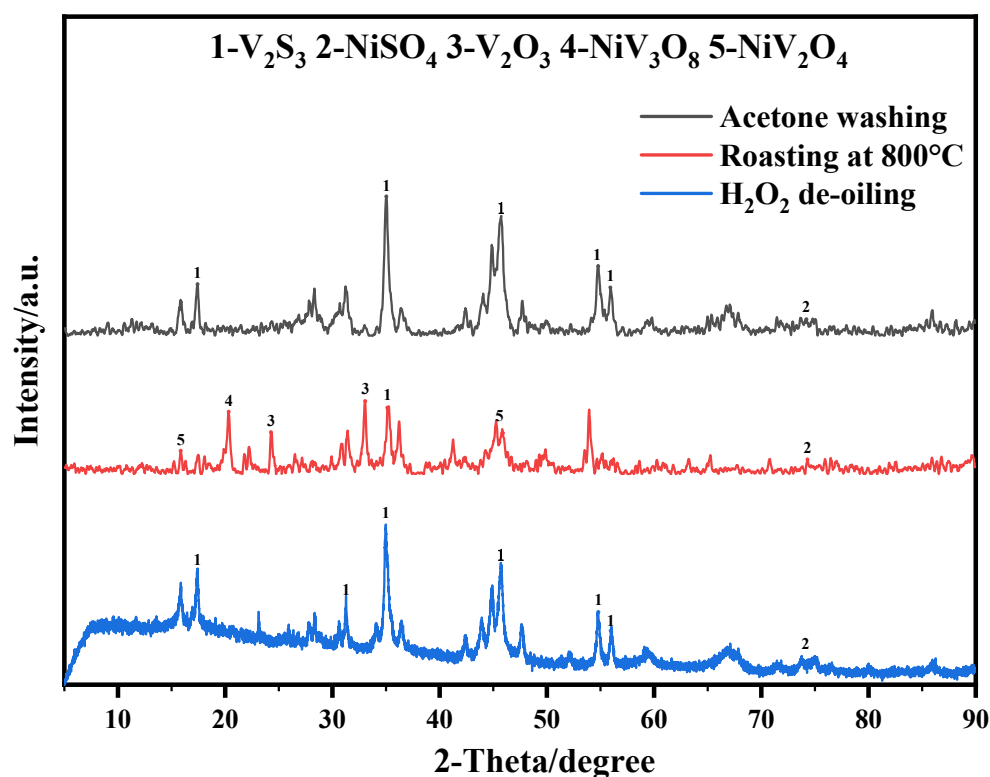


Figure 5. XRD patterns of the spent RHDP catalysts after different treatments.

3.2. Oxidative Leaching with Sodium Persulfate

The leaching experiments were carried out in the concentration range of 0.1–0.7 M, and in all experiments, the reaction temperature was 60 °C. As shown in Figure 6, when the $Na_2S_2O_8$ concentration was increased from 0.1 M to 0.5 M, the leaching efficiencies of vanadium and Al increased simultaneously. However, further increasing the $Na_2S_2O_8$ concentration to 0.7 M, the leaching efficiency of vanadium and Al decreased. Based on stoichiometry, 0.02198 mmol of $Na_2S_2O_8$ is required to oxidize V_2S_3 in 1 g of the sample completely. The 50 mL solution contains 0.025 mol $Na_2S_2O_8$. So, the excessive $Na_2S_2O_8$ makes the pH decrease to 2. In the pH range of 1.5–2, the high concentration of VO^{2+} in the solution is converted to V_2O_5 and precipitates out of the solution [26], which leads to a decrease in the leaching efficiency of vanadium. The decrease in the leaching efficiency of aluminum after the concentration of $Na_2S_2O_8$ exceeded 0.5 M was also related to this effect, because the deposition of V_2O_5 influences the further dissolution of aluminum. For this reason, the remaining tests were conducted at a $Na_2S_2O_8$ concentration of 0.5 M.

The effect of reaction temperature on the leaching efficiency was tested in the range of 40 °C to 90 °C. As shown in Figure 7, the metal-leaching efficiency was positively correlated with temperature. It is noteworthy that the leaching efficiency of Al increased slowly during the temperature increase from 40 to 70 °C. However, the leaching efficiency increased rapidly after the system temperature was over 80 °C. The high concentration of Al ions in the leachate will lead to a difficult separation and purification process. The solution pH was 1.13 after the reaction. It is supposed that the higher temperature and lower pH will lead to the dissolution of the Al_2O_3 carrier significantly.

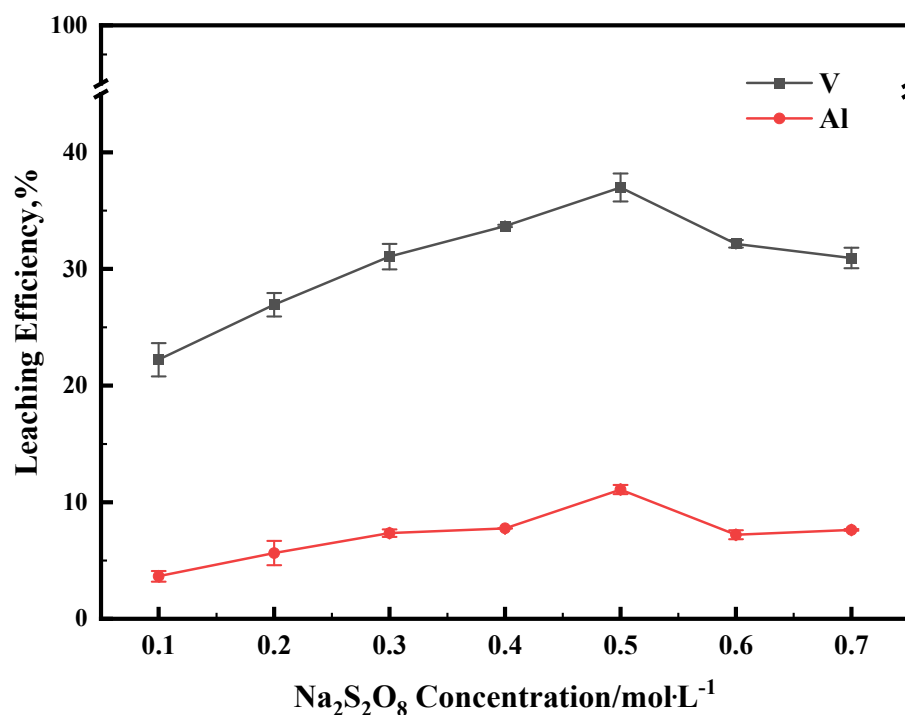


Figure 6. The effect of Na₂S₂O₈ concentration on leaching efficiency for V and Al. This experiment was run at 60 °C for 1 h.

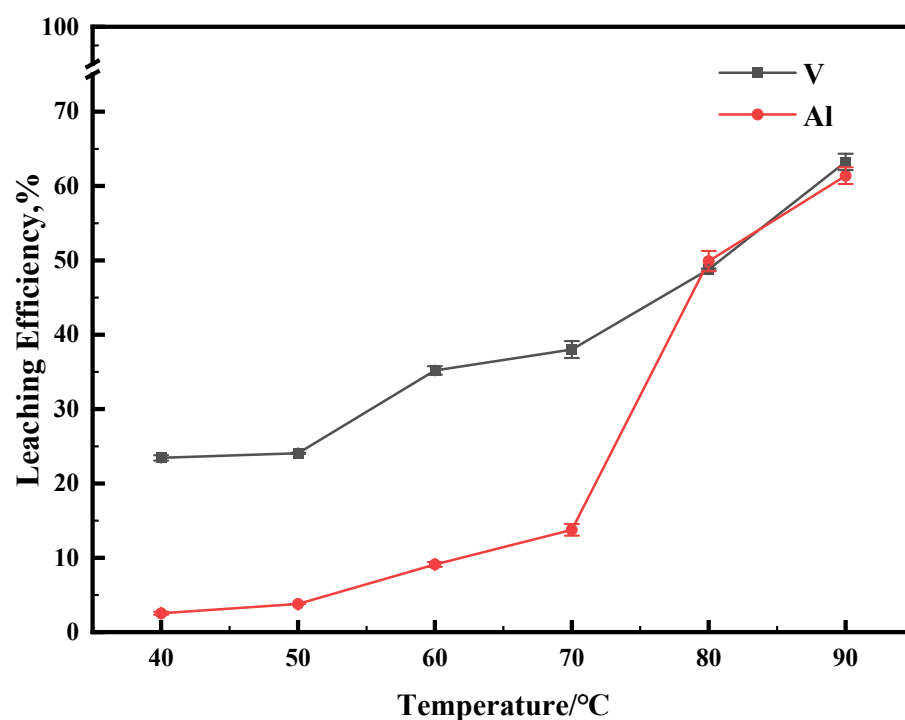


Figure 7. The effect of reaction temperature on leaching efficiency. This experiment was run for 1 h with concentration of 0.5 M of Na₂S₂O₈.

A series of experiments was performed at different initial pH values; the results are shown in Figure 8. The results showed that there was no obvious effect of the initial pH on the leaching efficiency of metals. According to the theory of the relationship between the form of vanadium in solution and the change in pH, at pH 1, when the concentration of vanadium is not very high, it exists mainly in the form of VO²⁺, and as the pH increases,

the form of V changes from VO^{2+} to $\text{V}_2\text{O}_5 \cdot x\text{H}_2\text{O}$ and polyvanadate and polyoxovanadate forms [25]. It can be observed in Figure 9 that metal sulfides react rapidly in $\text{Na}_2\text{S}_2\text{O}_8$ solutions, requiring only a short time to drop the pH of the system to below 2. In the cases of an initial pH of 3, 5, and 7, the pH of the system decreased to below 2 in a shorter period of time. Low pH allows vanadium to exist in a high valence state, which facilitates obtaining the product V_2O_5 but leads to more dissolution of the Al_2O_3 carrier.

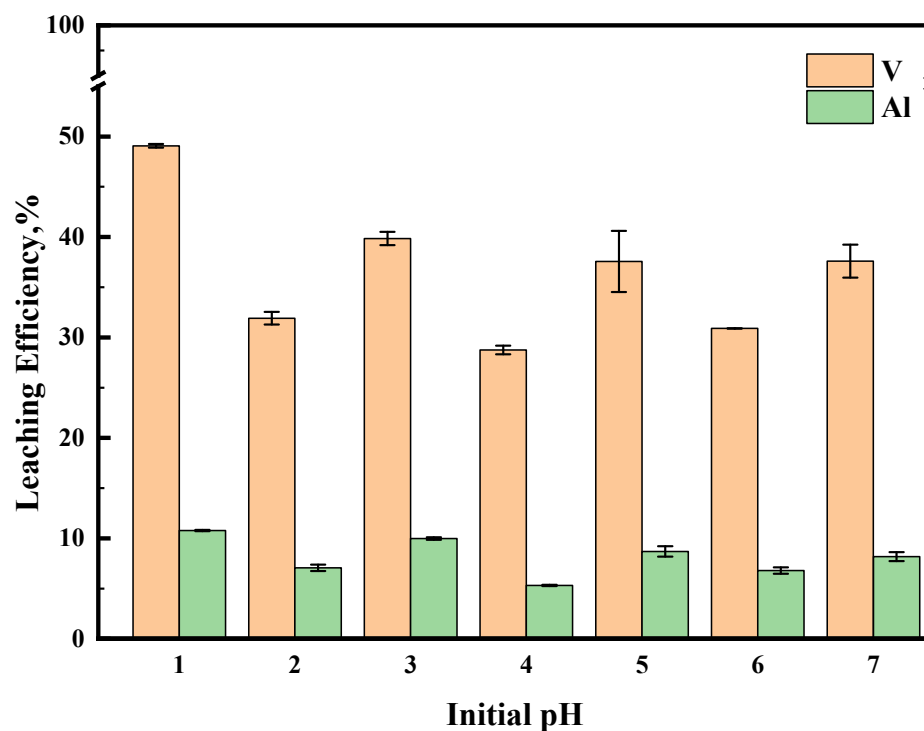


Figure 8. The effect of initial pH on leaching efficiency. This experiment was run at 70 °C for 1 h with concentration of 0.5 M of $\text{Na}_2\text{S}_2\text{O}_8$.

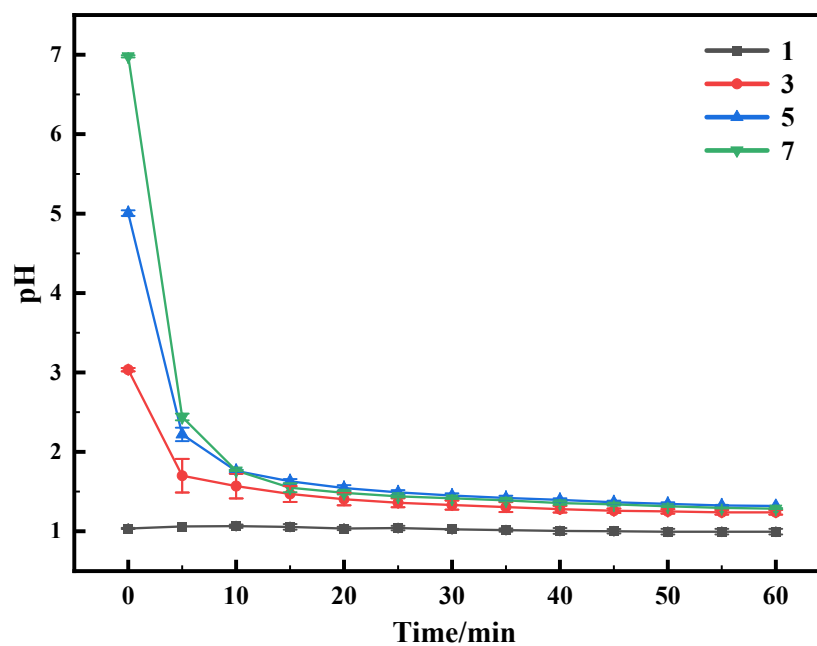


Figure 9. Graph of pH as a function of time. This experiment was run at 70 °C for 1 h with concentration of 0.5 M of $\text{Na}_2\text{S}_2\text{O}_8$.

The effect of reaction time on the leaching efficiency was investigated in a range of 1–5 h at a reaction temperature of 70 and 80 °C, while other experimental conditions were kept constant. As shown in Figure 10, when the reaction time was increased from 1 h to 3 h, the leaching efficiency of Al increased significantly, while the leaching efficiency of vanadium increased slowly. When the reaction time continued to be extended to 5 h, the leaching efficiency of vanadium increased rapidly to 78%. The results indicated that the extended reaction time was beneficial to the leaching of vanadium. However, the low pH value would lead to the gradual dissolution of the Al_2O_3 carrier, which would negatively affect the subsequent solid–liquid separation and the purification of vanadium. Therefore, the optimal reaction time should be reselected according to the reaction temperature.

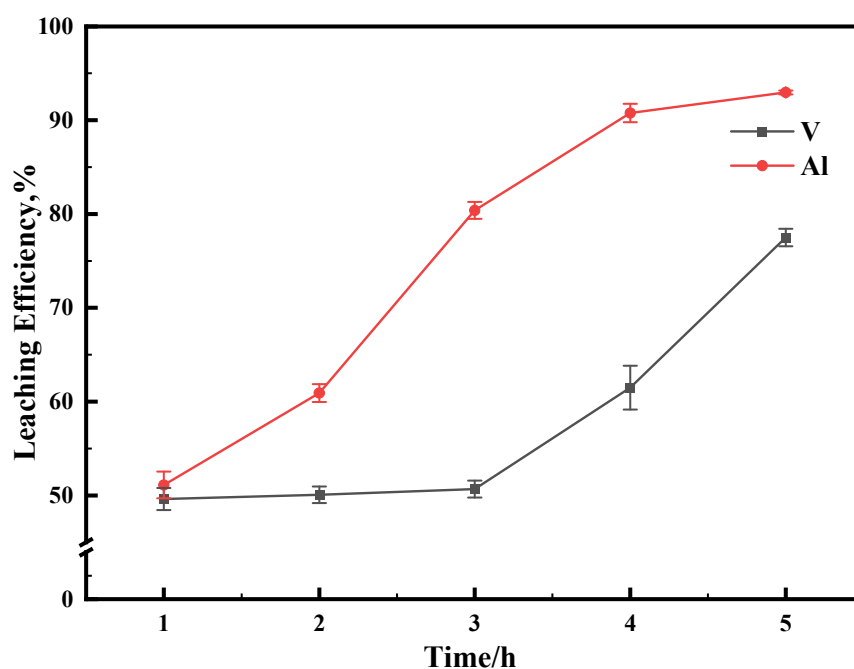


Figure 10. The effect of reaction time on leaching efficiency. This experiment was run at pH 3.05 and 80 °C for 1 h with concentration of 0.5 M of $\text{Na}_2\text{S}_2\text{O}_8$.

In order to inhibit the dissolution of carrier Al_2O_3 as much as possible, a milder oxidation condition was chosen according to the experimental conclusion. The reaction was carried out under relatively mild conditions (70 °C, 0.5 M $\text{Na}_2\text{S}_2\text{O}_8$) for 5 h, and the leaching results are shown in Figure 11. Under these conditions, the leaching efficiency of aluminum can be controlled to less than 15%.

3.3. Surface Analysis

In order to explore the limiting factors of the oxidative leaching reaction and further improve the leaching efficiency of vanadium, residue with different reaction times was selected for surface and physical phase analysis by using SEM and XRD, and the results are shown in Figures 12 and 13.

Figure 12 shows that many granules formed on the surface of the spent catalyst after oxidation. The EDS result showed that these granules are elemental sulfur.

The mechanism of metal sulfide dissolution and sulfur production is determined by the structure and chemical properties of the mineral [27]. Pyrite (FeS_2), molybdenite (MoS_2), and tungsten (WS_2) ore are acid-insoluble metal sulfides, and their oxidation follows the thiosulfate pathway. These metal sulfides have special valence bands that resist proton attack, and their chemical bond can only be broken by multi-step electron transfer with the oxidizing agent. For example, FeS_2 first produced the intermediate product thiosulfate

($S_2O_3^{2-}$) in the presence of an oxidizing agent. Subsequently, $S_2O_3^{2-}$ is further oxidized to sulfate (SO_4^{2-}) in a cyclic process.

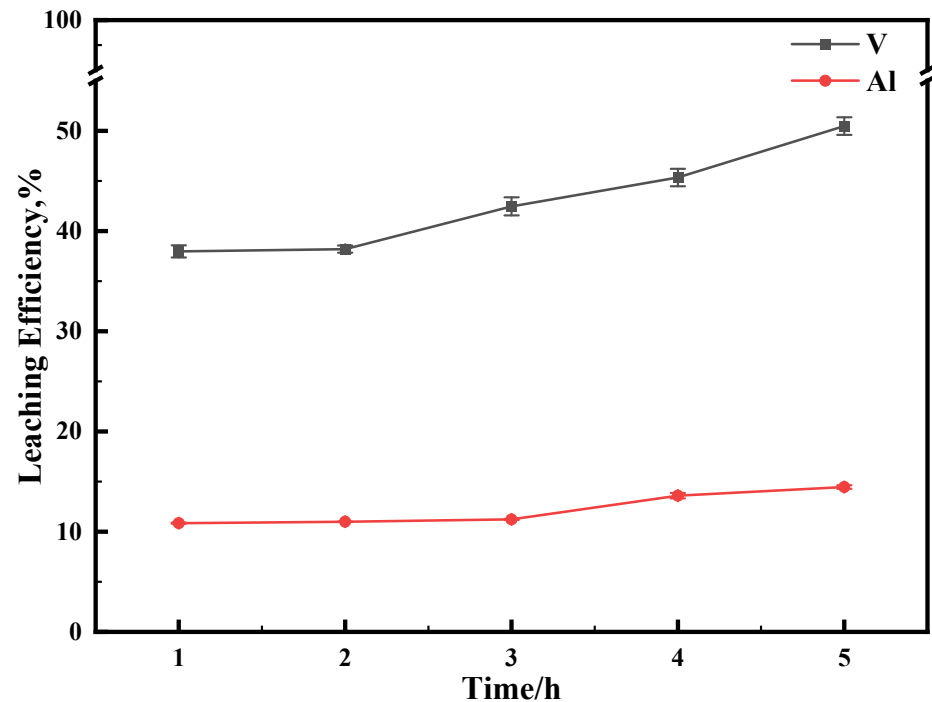


Figure 11. The effect of reaction time on leaching efficiency. This experiment was run at 70 °C for 1 h with concentration of 0.5 M of $Na_2S_2O_8$.

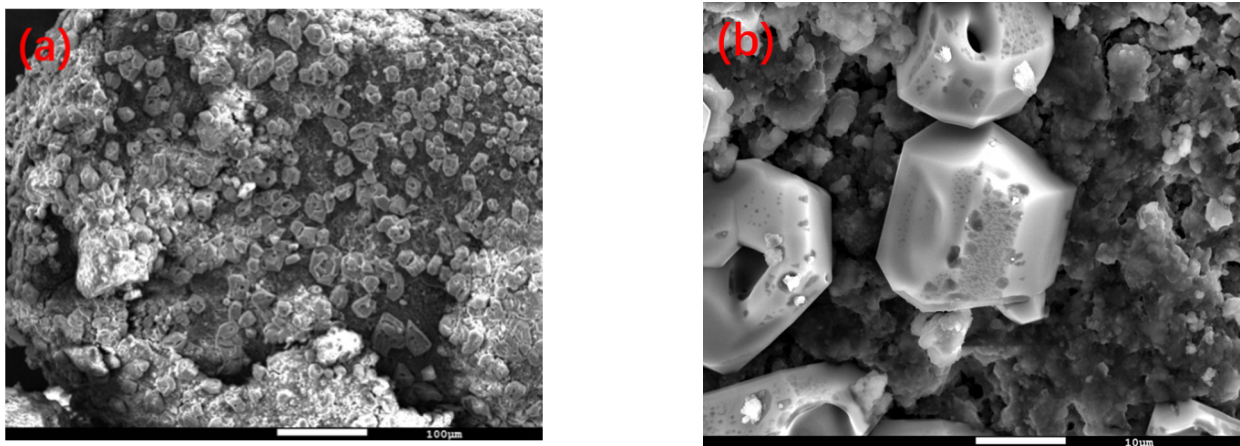


Figure 12. SEM images of the $Na_2S_2O_8$ oxidative leach residue. (a) Zoom magnification is 200 (b) Zoom magnification is 2000. This experiment was run at 70 °C for 2 h with concentration of 0.5 M of $Na_2S_2O_8$.

In contrast, the oxidation of acid-soluble metal sulfides is represented by sphalerite (ZnS) and orpiment (As_2S_3) which follow the polysulfide pathway.

The metal sulfide, under the attack of the proton, and the chemical bond of M-S break to generate M^{2+} and H_2S ; then, under the action of oxidant, H_2S is stepwise converted into polysulfide (H_2S_n). In an acidic solution, the polysulfide (H_2S_n) decomposes under the further action of the oxidizing agent, releasing elemental sulfur. S reacts slowly with H_2O in an oxygen atmosphere to form sulfate. However, it was reported that elemental sulfur could exist in an acidic solution containing persulfate and that elemental sulfur is very

stable below 393 K in an acid solution [23,28]. V_2S_3 is an acid-soluble metal sulfide, and its oxidation follows the polysulfide pathway.

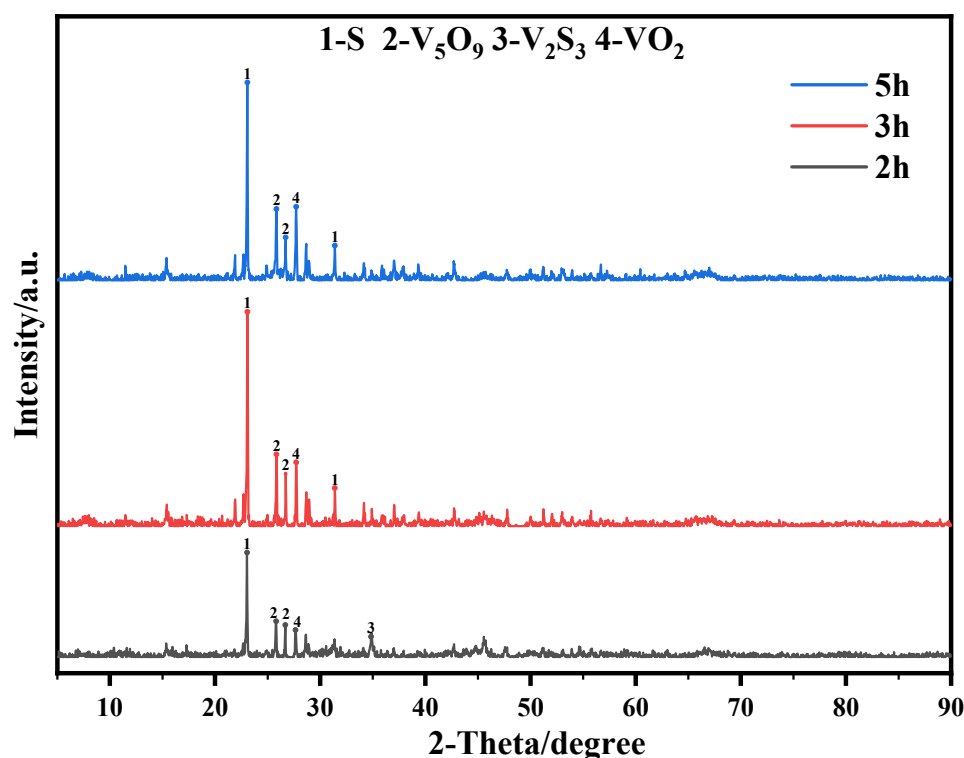


Figure 13. The XRD pattern of the oxidative leaching residue. This experiment was run at 70 °C for 2 h with concentration of 0.5 M of $Na_2S_2O_8$.

It can be seen that the intensity of the vanadium sulfide diffraction peaks in the oxidized leach residue gradually decreased with increasing reaction time while new vanadium oxide diffraction peaks were identified. In addition, S diffraction peaks were found in the XRD pattern of the oxidized leach residue, while the most obvious S diffraction peaks were found in the 5 h leach residue pattern. According to the following reaction:



The V_2S_3 in the spent catalyst is dissolved and consumed until it disappears entirely. V_2S_3 reacts with the oxidant to produce VO^{2+} and S. The high concentration of VO^{2+} in the solution will be gradually converted to V_2O_5 or other vanadium oxides under acidic conditions and then precipitated from the solution. At the same time, S will be deposited on the surface of the spent catalyst. The comprehensive analysis shows that the low leaching efficiency of vanadium is related to the fact that the vanadium oxide generated by the reaction is to dissolve incompletely in the acidic leaching solution.

3.4. Alkaline Leaching

For further improving the leaching efficiency of vanadium, the residue of the oxidizing experiment was leached under alkaline conditions with initial pHs of 9, 10, 11, 12, and 14, respectively. As seen in Figure 14, the leaching efficiency of vanadium gradually increased from 4.12% as the pH of the leachate increased from 9 to 14 and reached a maximum of 45.82% at pH 14. At the same time, aluminum was hardly leached when the pH of the leachate was 9–12. When the pH of the leachate increased to 14, the leaching efficiency of aluminum rapidly increased to 6.69%. So far, the experimental results can prove that the leaching efficiency of vanadium was increased by secondary alkaline leaching after being oxidized by $Na_2S_2O_8$. However, the high pH will lead to a considerable dissolution

of the carrier Al_2O_3 . Therefore, the selective leaching of vanadium and aluminum should be carried out under the preferred pH 12. At this point, the alkaline leaching efficiencies of vanadium and aluminum are 40.44% and 0.29%, respectively, and accounting for the results of oxidative leaching, it can be concluded that the leaching efficiency of vanadium reaches 90.92%. In comparison, the leaching efficiency of aluminum does not exceed 15%.

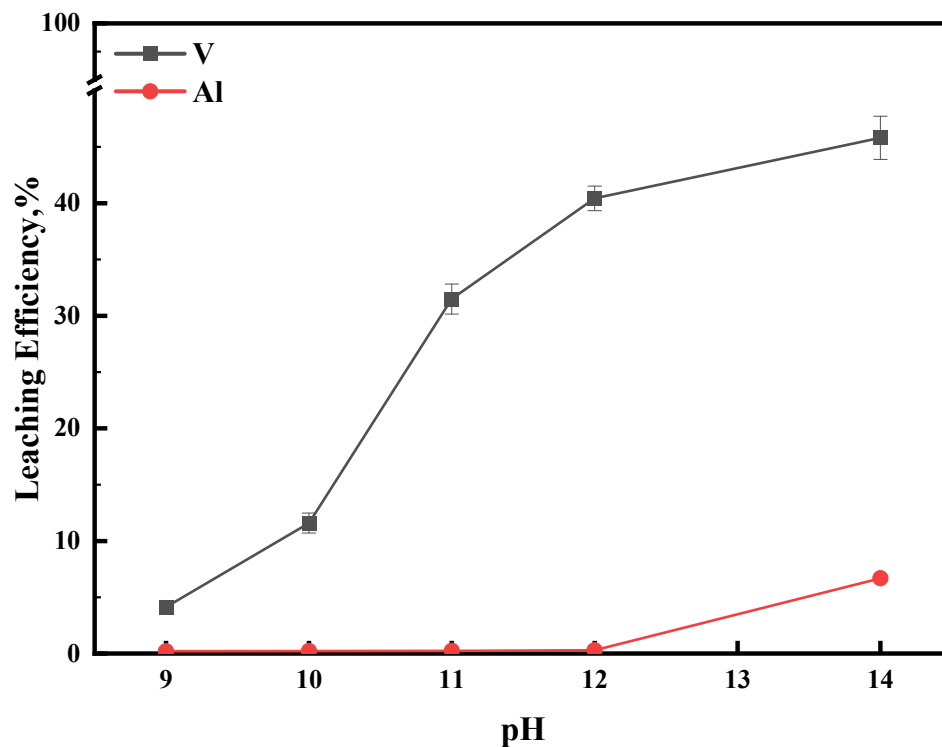


Figure 14. Effect of pH on alkali leaching efficiency. This experiment was run at 80 °C for 1 h.

The elemental content of the alkaline leaching residue was measured by XRF, and the results are shown in Table 2. It can be seen that the vanadium content of the alkaline leaching residue decreased with enhanced pH. When the pH increases to 12, a significant amount of sulfur and aluminum is retained in the leach residue, containing only 1.78% vanadium.

Table 2. XRF analysis of Alkaline leaching residue. This experiment was run at 80 °C for 1 h.

Leaching Conditions	Composition of Leaching Residue, wt%			
	O	S	V	Al
pH 9	54.82	26.43	5.66	10.72
pH 10	54.57	25.48	5.62	12.11
pH 11	54.47	25.00	4.77	13.50
pH 12	54.92	25.19	1.78	16.53
pH 14	54.64	25.75	2.16	14.55

The diffraction peaks of S and vanadium oxides were confirmed in the XRD spectrum of the alkaline leach residue (Figure 15).

The management of residues must reduce their heavy metal content. The alkaline leaching residue was mainly composed of Al_2O_3 and contained less than 2% vanadium, so the leaching residue is more readily available for further treatment, such as solidification and landfill [29].

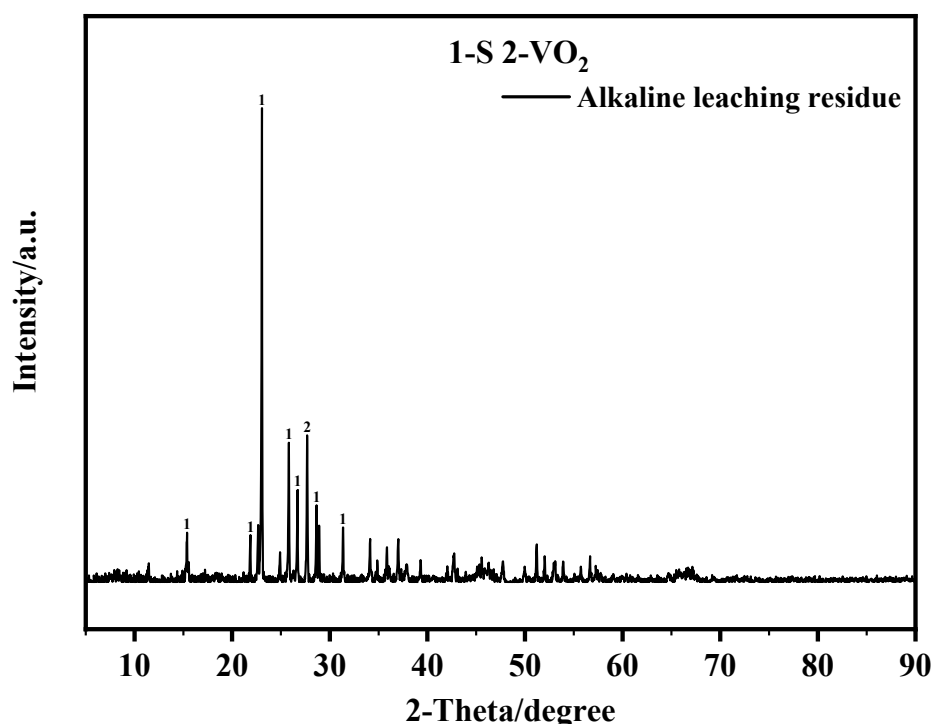


Figure 15. The XRD pattern of the alkaline leaching residue. This experiment was run at 80 °C for 1 h with a pH value at 12.

4. Conclusions

In this work, the surface-deposited vanadium was efficiently recovered from spent RHDP catalysts through the Fenton-like reaction followed by alkaline leaching. After de-oiling, the drop contact angle on the surface of the spent catalyst decreased from 147.3° to 89.8°, indicating that its surface properties changed to be hydrophilic. This transformation facilitates metal leaching. Through the comprehensive oxidation-alkali leaching process, under optimal conditions (oxidation was run at 70 °C in 5 h with a $\text{Na}_2\text{S}_2\text{O}_8$ concentration of 0.5 M; alkali leaching at 80 °C in 1 h), vanadium in the alkaline leaching residue was significantly reduced, and the removal efficiency of vanadium reached 90.92%. These results provide a proactive, green, simple approach for sustainable oil removal and recovery of valuable metals from spent residuum hydroprocessing catalysts under a relatively mild condition.

Author Contributions: Conceptualization, G.Z. (Guangji Zhang); Data curation, Y.L.; Formal analysis, G.Z. (Ge Zhao), C.S. and Y.C.; Investigation, Y.L.; Project administration, C.Y.; Supervision, Y.F.; Writing—original draft, Y.L.; Writing—review and editing, G.Z. (Guangji Zhang). All authors have read and agreed to the published version of the manuscript.

Funding: This study was financially supported by the Natural Science Foundation of China (NSFC21477165) and K. T. Li Foundation for Development of Science and Technology.

Data Availability Statement: The authors confirm that the data supporting the findings of this study are available within the article.

Conflicts of Interest: The authors declare no conflict of interest.

References

1. Kaufmann, T.G.; Kaldor, A.; Stuntz, G.F.; Kerby, M.C.; Ansell, L.L. Catalysis science and technology for cleaner transportation fuels. *Catal. Today* **2000**, *62*, 77–90. [[CrossRef](#)]
2. Haandel, L.V.; Bremmer, M.; Kooyman, P.J.; Veen, J.; Hensen, E. Structure-activity correlations in hydrodesulfurization reactions over Ni-promoted $\text{Mo}_x\text{W}_{1-x}\text{S}_2/\text{Al}_2\text{O}_3$ catalysts. *ACS Catal.* **2015**, *5*, 7276–7287. [[CrossRef](#)]
3. Hubaut, R. Vanadium-based sulfides as hydrotreating catalysts. *Appl. Catal. A-Gen.* **2007**, *322*, 121–128. [[CrossRef](#)]

4. Gao, F.; Olayiwola, A.U.; Liu, B.; Wang, S.; Du, H.; Li, J.; Wang, X.; Chen, D.; Zhang, Y. Review of Vanadium Production Part I: Primary Resources. *Min. Proc. Ext. Met. Rev.* **2022**, *43*, 466–488. [[CrossRef](#)]
5. Bian, Z.; Feng, Y.; Li, H.; Zhang, Y. New understanding of extraction and separation of vanadium (IV), iron and titanium using iron powder induction-leaching and P204-P507 synergistic extraction. *Sep. Purif. Technol.* **2022**, *288*, 120627. [[CrossRef](#)]
6. Wang, J.; Wang, S.; Olayiwola, A.; Yang, N.; Liu, B.; Weigand, J.; Wenzel, M.; Du, H. Recovering valuable metals from spent hydrodesulfurization catalyst via blank roasting and alkaline leaching. *J. Hazard. Mater.* **2021**, *416*, 125849. [[CrossRef](#)] [[PubMed](#)]
7. Petranikova, M.; Tkaczyk, A.H.; Bartl, A.; Amato, A.; Lapkovskis, V.; Tunsu, C. Vanadium sustainability in the context of innovative recycling and sourcing development. *Waste Manag.* **2020**, *113*, 521–544. [[CrossRef](#)] [[PubMed](#)]
8. Meshram, P.; Abhilash; Pandey, B.D. Advanced Review on Extraction of Nickel from Primary and Secondary Sources. *Min. Proc. Ext. Met. Rev.* **2019**, *40*, 157–193. [[CrossRef](#)]
9. Rout, P.C.; Mishra, G.K.; Padh, B.; Suresh, K.R.; Reddy, B.R. Solvent extraction separation of molybdenum as thio-molybdate complex from alkaline tungsten leach liquor of spent HDS catalyst—A pilot study. *Hydrometallurgy* **2017**, *174*, 140–146. [[CrossRef](#)]
10. Le, M.N.; Lee, M.S. A Review on Hydrometallurgical Processes for the Recovery of Valuable Metals from Spent Catalysts and Life Cycle Analysis Perspective. *Proc. Ext. Met. Rev.* **2021**, *42*, 335–354. [[CrossRef](#)]
11. Zhang, C.; Liu, X.; Liu, T.; Jiang, Z.; Li, C. Optimizing both the CoMo/Al₂O₃ catalyst and the technology for selectivity enhancement in the hydrodesulfurization of FCC gasoline. *Appl. Catal. A-Gen.* **2019**, *575*, 187–197. [[CrossRef](#)]
12. Feng, C.; Zhang, C.; Yuan, S.; Liu, M.; Chen, R.; Hu, H. Sustainable recovery of surface-deposited oils and valuable metals from uncrushed spent hydroprocessing catalysts. *J. Clean. Prod.* **2022**, *338*, 130564. [[CrossRef](#)]
13. Ye, X.; Guo, S.; Qu, W.; Yang, L.; Hu, T.; Xu, S.; Zhang, L.; Liu, B.; Zhang, Z. Microwave field: High temperature dielectric properties and heating characteristics of waste hydrodesulfurization catalysts. *J. Hazard. Mater.* **2019**, *366*, 432–438. [[CrossRef](#)] [[PubMed](#)]
14. Ruiz, V.; Meux, E.; Diliberto, S.; Schneiders, M. Hydrometallurgical Treatment for Valuable Metals Recovery from Spent CoMo/Al₂O₃ Catalyst. 1. Improvement of Soda Leaching of an Industrially Roasted Catalyst. *Ind. Eng. Chem. Res.* **2011**, *50*, 5295–5306. [[CrossRef](#)]
15. Barik, S.P.; Park, K.H.; Parhi, P.K.; Park, J.T. Direct leaching of molybdenum and cobalt from spent hydrodesulphurization catalyst with sulphuric acid. *Hydrometallurgy* **2012**, *111*, 46–51. [[CrossRef](#)]
16. Zhang, D.; Liu, Y.; Hu, Q.; Ke, X.; Hu, J. Sustainable recovery of nickel, molybdenum, and vanadium from spent hydroprocessing catalysts by an integrated selective route. *J. Clean. Prod.* **2019**, *252*, 119763. [[CrossRef](#)]
17. Yang, Y.; Xu, S.; Li, Z.; Wang, J.; Zhao, Z.; Xu, Z. Oil removal of spent hydrotreating catalyst CoMo/Al₂O₃ via a facile method with enhanced metal recovery. *J. Hazard. Mater.* **2016**, *318*, 723–731. [[CrossRef](#)]
18. Mishra, D.; Chaudhury, G.R.; Kim, D.J.; Ahn, J.G. Recovery of metal values from spent petroleum catalyst using leaching-solvent extraction technique. *Hydrometallurgy* **2010**, *101*, 35–40. [[CrossRef](#)]
19. Gopinath, R.; Paital, A.R.; Patel, B.K. V₂O₅-H₂O₂: A convenient reagent for the direct oxidation of acetals to esters. *Tetrahedron. Lett.* **2002**, *43*, 5123–5126. [[CrossRef](#)]
20. Liu, J.; Wang, W.; Wang, L.; Jian, P. Heterostructured V₂O₅/FeVO₄ for enhanced liquid-phase epoxidation of cyclooctene. *J. Colloid. Interf. Sci.* **2023**, *630*, 804–812. [[CrossRef](#)]
21. Deng, J.; Jiang, J.; Zhang, Y. FeVO₄ as a highly active heterogeneous Fenton-like catalyst towards the degradation of Orange II. *Appl. Catal. B Environ.* **2008**, *84*, 468–473. [[CrossRef](#)]
22. Lai, L.; Zhou, P.; Zhou, H.; Sun, M.; Yuan, Y.; Liu, Y.; Yao, G.; Lai, B. Heterogeneous Fe(III)/Fe(II) circulation in FeVO₄ by coupling with dithionite towards long-lasting peroxymonosulfate activation: Pivotal role of vanadium as electron shuttles. *Appl. Catal. B Environ.* **2021**, *297*, 120470. [[CrossRef](#)]
23. Liu, Z.; Xiang, Y.; Yin, Z.; Wu, X.; Jiang, J.; Chen, Y.; Xiong, L. Oxidative leaching behavior of metalliferous black shale in acidic solution using persulfate as oxidant. *Trans. Nonferrous Met. Soc. China* **2016**, *26*, 565–574. [[CrossRef](#)]
24. Arslanolu, H.; Yara, A. Recovery of molybdenum, cobalt and nickel from spent hydrodesulphurization catalyst through oxidizing roast followed by sodium persulfate leaching. *Sustain. Mater. Technol.* **2021**, *28*, e286. [[CrossRef](#)]
25. Schippers, A.; Sand, W. Bacterial leaching of metal sulfide proceeds by two indirect mechanisms via thiosulfate or via polysulfides and sulfur. *Appl. Environ. Microbiol.* **1999**, *65*, 319–321. [[CrossRef](#)]
26. Chen, R.; Feng, C.; Tan, J.; Zhang, C.; Yuan, S.; Liu, M.; Hu, H.; Li, Q.; Hu, J. Stepwise separation and recovery of molybdenum, vanadium, and nickel from spent hydrogenation catalyst. *Hydrometallurgy* **2022**, *213*, 106910. [[CrossRef](#)]
27. Sand, W.; Gehrke, T.; Joza, P.; Schippers, A. (Bio)chemistry of bacterial leaching—Direct vs. indirect bioleaching. *Hydrometallurgy* **2001**, *59*, 159–175. [[CrossRef](#)]
28. Xue, J.; Lu, X.; Du, Y.; Mao, W.; Wang, Y.; Li, J. Ultrasonic-assisted Oxidation Leaching of Nickel Sulfide Concentrate. *Chin. J. Chem. Eng.* **2010**, *18*, 948–953. [[CrossRef](#)]
29. Rao, F.; Liu, Q. Geopolymerization and Its Potential Application in Mine Tailings Consolidation: A Review. *Min. Proc. Ext. Met. Rev.* **2015**, *36*, 399–409. [[CrossRef](#)]

Disclaimer/Publisher's Note: The statements, opinions and data contained in all publications are solely those of the individual author(s) and contributor(s) and not of MDPI and/or the editor(s). MDPI and/or the editor(s) disclaim responsibility for any injury to people or property resulting from any ideas, methods, instructions or products referred to in the content.